Influence of different biomass ash additive on anthracite pyrolysis process and char gasification reactivity

Xiaoming Li[1] · Caifeng Yang[1] · Mengjie Liu[2,3] · Jin Bai[2] · Wen Li[2]

Abstract Catalytic coal gasification technology shows prominent advantages in enhancing coal gasification reactivity and is restrained by the cost of catalyst. Two typical biomass ash additions, corn stalk ash (CSA, high K–Na and low Si) and poplar sawdust ash (PSA, high K–Ca and high Si), were employed to study the influence of biomass ash on pyrolysis process and char gasification reactivity of the typical anthracite. Microstructure characteristics of the char samples were examined by X-ray diffraction (XRD). Based on isothermal char-CO_2 gasification experiments, the influence of biomass ash on reactivity of anthracite char was determined using thermogravimetric analyzer. Furthermore, structural parameters were correlated with different reactivity parameters to illustrate the crucial factor on the gasification reactivity varied with char reaction stages. The results indicate that both CSA and PSA additives hinder the growth of adjacent basic structural units in a vertical direction of the carbon structure, and then slow down the graphitization process of the anthracite during pyrolysis. The inhibition effect is more prominent with the increasing of biomass ash. In addition, the gasification reactivity of anthracite char is significantly promoted, which could be mainly attributed to the abundant active AAEM (especially K and Na) contents of biomass ash and a lower graphitization degree of mixed chars. Higher K and Na contents illustrate that the CSA has more remarkable promotion effect on char gasification reactivity than PSA, in accordance with the inhibition effect on the order degree of anthracite char. The stacking layer number could reasonably act as a rough indicator for evaluating the gasification reactivity of the char samples.

Keywords Biomass ash · Catalytic effect · Pyrolysis · Gasification reactivity · Structural parameters · AAEM

✉ Jin Bai
  stone@sxicc.ac.cn

1 School of Chemical and Biological Engineering, Taiyuan University of Science and Technology, Taiyuan 030024, Shanxi, China

2 State Key Laboratory of Coal Conversion, Institute of Coal Chemistry, Chinese Academy of Sciences, Taiyuan 030001, China

3 University of Chinese Academy of Sciences, Beijing 100049, China

1 Introduction

Coal is the second largest resource in the word's primary energy consumption (Zhang et al. 2019), and then many efforts have been made to meet the increasing demand for clean and efficient coal utilization. Gasification is generally considered as the core technology for efficiently and cleanly utilizing carbonaceous materials (Xie et al. 2019), and advanced large-scale coal gasification has achieved widespread industrial application. However, with the development of coal gasification technology, the coal resource consumption and low efficiency caused by the specificity of coal type are gradually exposed. Accordingly, low gasification reactivity of anthracite results in restricted utilization, indicating that longer reaction time and higher

gasification temperature are necessary for reaching a higher carbon conversion. Therefore, it is of great significance to explore a novel gasification technology to optimize the allocation of resources and promote gasification efficiency of anthracite. Catalytic coal gasification technology and the co-gasification technology of coal and other carbonaceous materials have shown prominent effect on the gasification reaction rate of coal sample, which provides effective ways to promote the low gasification reactivity of anthracite (Kopyscinski et al. 2014; Wu et al. 2019). To achieve industrial application of co-gasification technology, it is necessary to make an in-depth understanding of the interaction mechanism between anthracite and additives.

Bioenergy has been gaining increased attention as an alternative and important carbon-containing renewable energy due to global warming problems originating mostly from the combustion of fossil fuels (Qin et al. 2017). Although the biomass has the merits of abundant source and CO_2 neutral, the disadvantages containing the high moisture content, the low energy density, inferior flowability and grindability inevitably lead to some technical and economic challenges for storage, handle, and conversion of biomass (Carpenter et al. 2014; Sermyagina et al. 2016; Zhang et al. 2016a, b). Recently, the co-pyrolysis characteristic of biomass and coal and the subsequent co-gasification reactivity have been widely studied to reveal the co-gasification mechanism, and then provide the theory basis of coal-biomass co-gasification (Qin et al. 2017; Wei et al. 2017a; Wu et al. 2019). The addition of biomass would affect the evolution of pore structure and increase the disordered degree of char during co-pyrolysis, which was also favorable for the subsequent gasification reaction (Wu et al. 2017). However, the differences in the volatile content and properties of coal and biomass have brought great challenges to understanding the effects of biomass ash on the co-pyrolysis and co-gasification of coal-biomass.

In addition, a number of researchers have studied the influence of catalysts on char structural evolution and gasification characteristics (Ding et al. 2015; Liu et al. 2017; Zheng et al. 2019; Zhou et al. 2018; Zhu et al. 2018). The utilization of catalysts can either improve the carbon conversion or reduce gasification temperature but keep the high conversion rate (Karimi and Gray 2011; Rizkiana et al. 2014a). Alkali and alkaline earth metals (AAEMs) and transition metals catalyst could promote the gasification rate by changing the physicochemical structure of char, which have also been widely accepted as a common sense (Huang et al. 2009). However, the commercially catalytic coal gasification projects were limited by the secondary pollution of catalyst and the expensive costs of industrial catalyst design, manufacture and recovery (Fernandes et al. 2017; Wei et al. 2017b). Therefore, it is

imperative to find a cheap and environment-friendly coal gasification catalyst for the gasification process.

Biomass ash, the solid residue of biomass combustion and gasification, is a huge potential industrial catalysts (Fernandes et al. 2017; Masnadi et al. 2015), which can be attributed to the high output of biomass and high AAEMs contents of biomass (Satyam Naidu et al. 2016). Approximate 95% of biomass resources is used directly for burning, the corresponding global biomass ash output per year is about 476 million tonners (Vassilev et al. 2013). Therefore, the utilization of biomass ash as industrial catalyst in the coal gasification process is not only beneficial for dealing with the solid residue and reducing the environment risks, but it also overcome the above-stated disadvantage of industrial catalyst and then promote gasification efficiency. However, there are few investigations on the influence of biomass ash on the process of coal pyrolysis and char gasification reactivity. Moreover, the chemical composition and concentration of biomass ash additive varied with the type and mass ratio in the mixture char. It is required to understand the role of biomass ash in the coal pyrolysis and gasification process, which can provide the evidence for biomass ash as a promising industrial catalyst and more precise knowledge for co-pyrolysis and co-gasification of coal-biomass.

The char structure, including pore structure (pore volume and specific surface area), alkali index, microcrystalline structure, and O-containing functional groups, is considered to be an essential factor affecting the gasification reactivity (Li et al. 2017; Qing et al. 2019). In spite of the relationship between reactivity indicators and the structural parameters of coal char under a specific gasification temperature has been widely studied, the structural models for predicting the gasification reactivity of char were restricted to the specific research conditions (Liu et al. 2020a). So far, there is no unified conclusion that whether there is an acceptable factor for evaluating gasification reactivity of different carbonaceous materials. The quantitative relationships between the structural parameters and reactivity of the char with different biomass ash additions was remain unclear. Therefore, it is very meaningful to establish reasonable correlation based on the structure parameters for predicting the gasification characteristics to reflect the effect of the addition of biomass ash on coal char reaction.

The aim of this paper is to clearly understand the influence of biomass ash on char structural characteristics and gasification reactivity. The pyrolysis experiments of Shanxi anthracite with two typical biomass ash (corn stalk ash and poplar sawdust ash) were performed in a fixed bed reactor. The XRD was used to evaluate the microstructure characteristics of different char samples. Meanwhile, TGA was employed to estimate the gasification reactivity of char

samples at gasification temperature of 900 °C. The excellent linear correlations between microstructure of char samples and different gasification reactivity parameters were established. This investigation will reveal the catalytic role and reaction mechanism of AAEM in the biomass ash additive, which provide the basis of biomass ash as cheap industrial catalysts on coal pyrolysis and gasification.

2 Experimental materials and methods

2.1 Preparation of biomass ash and mixed coal sample

Two biomass samples, corn stalk (denoted as CS) and poplar sawdust (denoted as PS) derived from Shanxi province, were used in this work. Biomass sample was dried at 50 °C for 12 h, and then it was crushed and sieved to a particle size of 150–180 μm. The preparation of biomass ash was carried out on the basis of Chinese National Standards of GB/T 30725–2014. The detailed procedures as follows: the biomass sample was put into the muffle, then heat it from room temperature to 255 °C with the heating rate of 5 °C/min in air atmosphere. After that, holding at 255 °C for1 h, then heating up to 500 °C and keeping for 2 h. Afterward, biomass ash was cooled to room temperature.

An anthracite (denoted as AC), from Jincheng, Shanxi Province, was dried and grounded to a particle size of 120–150 μm. Prior to pyrolysis experiments, the biomass ash was evenly and sufficiently blended with AC sample by mechanical mixing method in mortar. The mass ratios of biomass ash in the mixtures were 20%, 50% and 80%, respectively. The corresponding char samples were named on the basis of the type and mass ratio of biomass ash. For instance, AC-CSA20% represented that the blend was AC coupled with CSA of 20%. Proximate and ultimate analyses of the coal and biomass samples, and chemical compositions of coal and biomass ash are shown in Tables 1 and 2, respectively. It could be obviously seen that CSA had high contents of potassium and sodium, while PSA had high contents of potassium, silicon and calcium, which revealed that two biomass ashes had significant differences in chemical compositions.

2.2 Preparation of different char samples

The AC and mixed coal samples were pyrolyzed in a fixed bed reactor. About 5 g of coal sample was carefully placed into the silica tube reactor and the continuous high-purity nitrogen (200 mL/min) was then fed into the reactor. After keeping for 30 min to remove the air, the temperature was heated up to 600 °C at a constant heating rate of 10 °C/min, and then hold for 60 min to remove most of the volatile matter before dropping to room temperature. Afterward, the char sample was collected and pulverized below 75 μm for subsequent experiments. Figure 1 illustrates the whole experimental procedure and analysis methods for the structural characteristics and gasification reactivity of the char samples.

Table 1 Proximate and ultimate analyses of AC and biomass samples

Sample	Proximate analysis (wt%)				Ultimate analysis (d, wt%)				
	M_{ad}	A_d	V_{daf}	FC_d	C	H	O^a	N	S
AC	0.80	25.19	14.00	64.33	66.43	2.98	3.28	1.18	0.34
CS	4.98	5.01	80.58	18.45	43.8	5.09	40.77	0.42	0.18
PS	1.35	1.60	84.31	15.44	48.21	6.01	42.7	0.14	0.01

ad: air dried basis; d: dry basis; daf: dry ash-free basis; [a]: By difference

Table 2 Chemical compositions of AC and biomass ash additives (wt%)

Sample	SiO_2	Al_2O_3	Fe_2O_3	CaO	MgO	SO_3	TiO_2	K_2O	Na_2O	P_2O_5
ACA	49.11	29.02	12.04	3.91	0.50	2.36	1.91	0.52	0.51	0.12
CSA	27.01	0.86	0.43	7.95	12.01	7.54	0.05	35.91	2.39	5.86
PSA	53.44	3.07	0.69	15.03	7.08	N/A	0.18	12.51	0.54	N/A
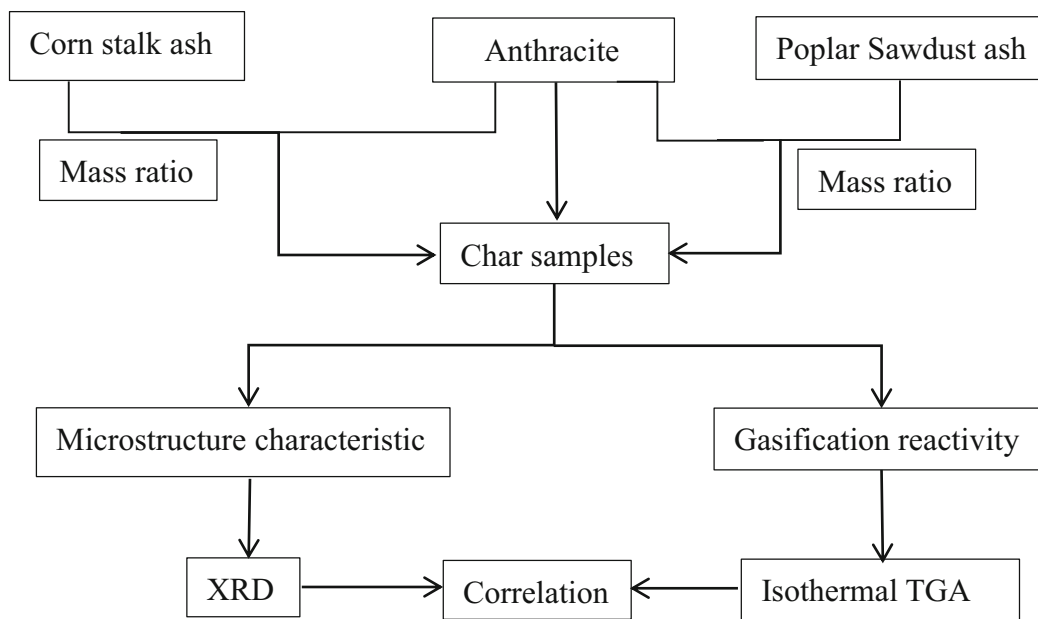
Fig. 1 Experimental procedure and analysis methods for the structure and gasification reactivity of the char samples

Fig. 2 XRD spectrum of different char samples at 600 °C: **a** AC-CSA char, **b** AC-PSA char

2.3 X-ray diffraction analysis

As a non-destructive and good reproducibility technique, XRD is one of the most widely employed means for analyzing the microcrystalline structure of the char samples. The PANalytical X'pert3 diffractometer with Cu Kα radiation (the wavelength $\lambda = 1.5406$ Å) was applied to determine the evolution in the microcrystalline structure. The operating electric current and voltage of the equipment were 40 mA and 40 kv, respectively. The char sample was placed in a rectangular glass groove and flattened by glass sheets. Finally, it was scanned from a 2θ angle range of 10°–80° with a 0.02° step interval at a speed of 4°/min.

For further quantitatively analysis, the 002 peak was curve-fitted into two Guass bands of a relatively poorly-defined microcrystalline structure (P band at about 20°) and a relatively good microcrystalline structure (G band at about 26°) (Wu et al. 2008), which was shown in Fig. 2. The crystallite structure parameters could be calculated by using the following conventional Bragg's law and Scherrer equations (Bo et al. 2003):

$$d_{002.P} = \frac{\lambda}{2\sin\left(\theta_{002,P}\right)} \tag{1}$$

$$d_{002.G} = \frac{\lambda}{2\sin\left(\theta_{002,G}\right)} \tag{2}$$

$$L_{C.P} = \frac{0.94\lambda}{\beta_{002,P}\cos\left(\theta_{002,P}\right)} \tag{3}$$

$$L_{C.G} = \frac{0.94\lambda}{\beta_{002,G}\cos\left(\theta_{002,G}\right)} \tag{4}$$

where $d_{002,P}$ and $d_{002,G}$ represent the interplanar spacings of the P and G component, respectively. λ is the wavelength of the incident X-radiation used ($\lambda = 1.5406$ Å). Meanwhile, $2\theta_{002,P}$ and $2\theta_{002,G}$ are the diffraction angles of P and G peak. $L_{c,P}$ and $L_{c,G}$ are the corresponding stacking height, $\beta_{002,P}$ and $\beta_{002,G}$ mean the corresponding full width at half maximum (FWHM) of P and G peak.

On the basis of the relevant parameters of the P peak and the G peak, the ultimately overall results of the crystalline structure parameters of different char samples could be determined by the equations as follow (Liu et al. 2020a; Wu et al. 2008):

$$d_{002,a} = X_P d_{002,P} + X_G d_{002,G} \tag{5}$$

$$L_{c,a} = X_P L_{c,P} + X_G L_{c,G} \tag{6}$$

$$X_P = \frac{S_P}{S_P + S_G} \tag{7}$$

$$X_G = \frac{S_G}{S_P + S_G} \tag{8}$$

$$N = \frac{L_{c,a}}{d_{002,a}} \tag{9}$$

where, $d_{002,a}$ and $L_{c,a}$ are the average interplanar spacing and stacking height of the coal char samples, respectively; X_P is the fractions of the P part, and X_G is the fractions of the G part. Besides, S_P and S_G represent the band areas of the P and G part, respectively. N is the stacking layer number.

2.4 Gasification reactivity measurement of char samples

The carbon dioxide (CO_2) gasification reactivity of individual and mixed char samples were analyzed in a TGA (Setsys Evolution, SETARAM, France). The specific sequences were as follows: The sample (about 10 mg) was placed into alumina crucible, and then it was heated from 30 to 105 °C at the heating rate of 20 °C/min under N_2 atmosphere with the flow rate of 140 mL/min. After that, holding at 105 °C for 30 min, then it was heated up to 900 °C at 20 °C/min. Then, the N_2 was immediately switched to CO_2 flow of 140 mL/min to measure reactivity. Three repeated tests were performed to ensure the reproducibility of each experimental result, and the consequences revealed that the reproducibility was very good. The TGA results were modified by subtracting the predetermined baselines which were performed under the same condition with blank crucible. In this study, the internal and external diffusion have been eliminated. According to the TGA data, the CO_2 gasification carbon conversion (X_c) of the char samples can be calculated by the following function (Wei et al. 2017a):

$$X_c = \frac{m_0 - m_t}{m_0 - m_{ash}} \times 100\% \tag{10}$$

where, m_0 represents the initial mass of the char sample; m_t represents sample mass when gasification time reaches the reaction time t; and m_{ash} is the ash mass in the char sample.

The gasification rate r (%/h) is generally defined as the differential of carbon conversion to gasification reaction time:

$$r = \frac{dX_c}{dt} \tag{11}$$

To evaluate the gasification performance of char sample, the reactivity parameters R_{X_c} (h^{-1}) under different stages were defined as follows:

$$R_{X_c} = \frac{X_c}{\tau_{X_c}} \tag{12}$$

where, τ_{X_c} represents the required time when the carbon conversion of the char sample reaches X_c.

3 Results and discussion

3.1 Influence of biomass ash on microcrystalline structure of AC char sample

Figure 3 presents the XRD pattern of the AC char and mixed chars with different mass ratios of biomass ash additions. It could be observed that two evident peaks appeared at a 2θ angle range of 19°–24° and 42°–45°, which were attributed to 002 and 100 diffraction peaks in diffuse graphite of the char samples, respectively. A narrower and higher background intensity of 002 peak represented the more ordered carbon structure, higher degree of graphitization and less reactive sites on the surface of char samples. As shown in Fig. 3, the 002 peak of the AC char was the narrowest and highest, indicating that AC had the highest graphitization degree. With the rise of the proportion of biomass ash, the 002 peak intensity of AC-CSA char samples decreased from 6129 to 3604, while the 002 peak intensity of AC-PSA chars reduced to 4867. Meanwhile, the 002 peak gradually became broad shape and low intensity. The results demonstrated that the addition of both CSA and PSA could hinder the order degree of AC char, and the corresponding effect was more prominent with the increase of the proportion of biomass ash in mixed char sample. The inhibition effect of biomass ash on the graphitization process could be attributed to two aspects. The AAEM species are usually easily released from biomass ash during pyrolysis, indicating that AAEM may be combined with coal/char matrix and fixed on adjacent basic structural units (BSU), which destroys the parallelism of the layers and the stability of the interplanar spacing, thus
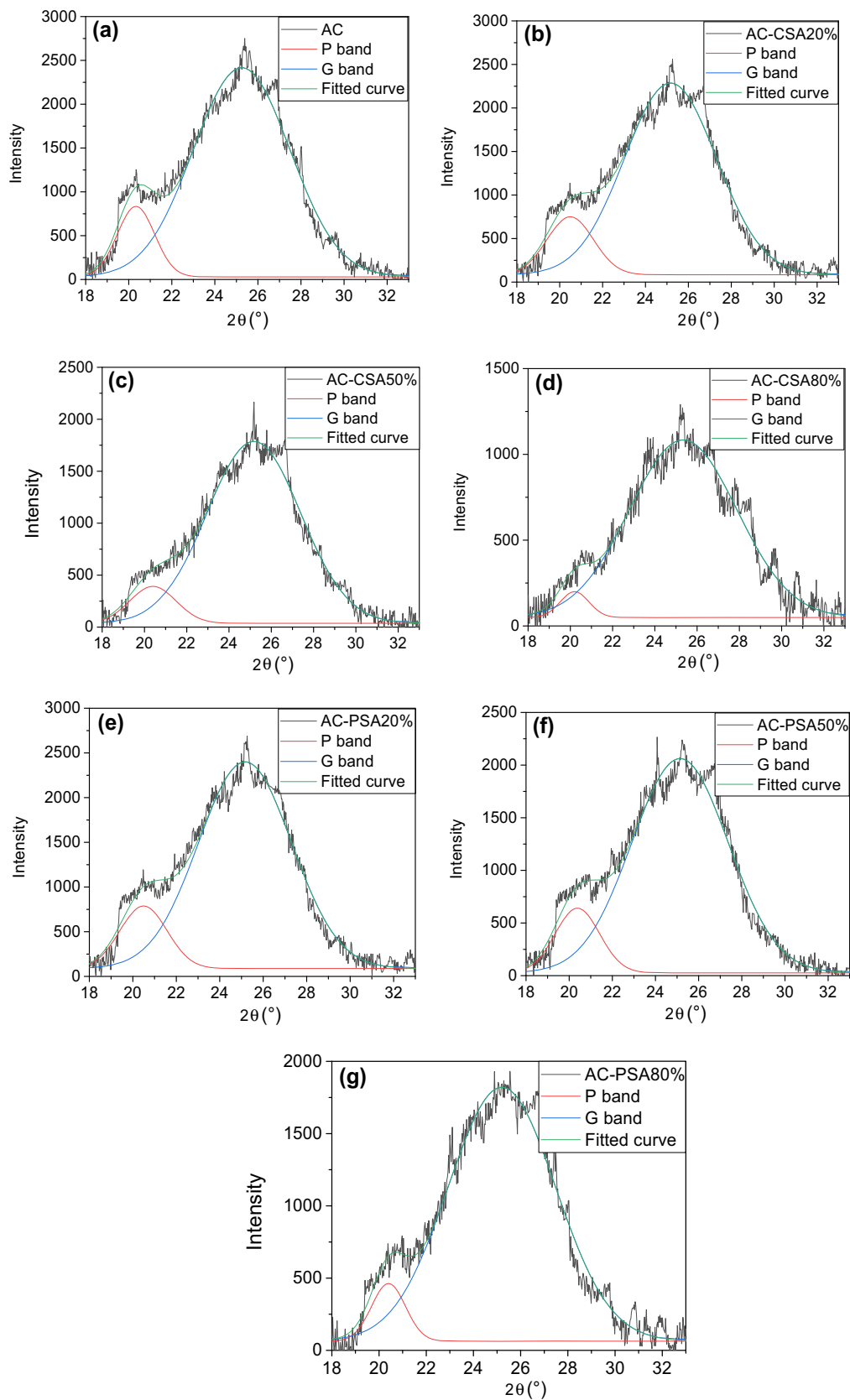
Fig. 3 Curve-fitting XRD spectrum of 002 peak for different char samples: **a** AC char, **b** AC-CSA20% char, **c** AC-CSA50% char, **d** AC-CSA80% char, **e** AC-PSA20% char, **f** AC-PSA50% char, **g** AC-PSA80% char

Table 3 Microcrystalline structural parameters of resulting char samples

Sample	$d_{002,P}$ (Å)	$L_{c,P}$ (Å)	$d_{002,G}$ (Å)	$L_{c,G}$ (Å)	X_P	X_G	$d_{002,a}$ (Å)	$L_{c,a}$ (Å)	N
AC	4.36	41.28	3.52	16.05	11.5	88.5	3.62	18.95	5.23
AC-CSA20%	4.33	33.01	3.54	16.79	13.2	86.8	3.62	18.59	5.13
AC-CSA50%	4.35	32.66	3.53	16.30	9.0	91.0	3.59	17.78	4.95
AC-CSA80%	4.39	52.84	3.51	14.16	3.7	96.3	3.56	15.61	4.39
AC-PSA20%	4.33	33.53	3.53	16.69	11.9	88.1	3.63	18.69	5.15
AC-PSA50%	4.35	34.80	3.54	16.12	12.1	87.9	3.63	18.38	5.06
AC-PSA80%	4.35	49.83	3.53	15.46	6.7	93.3	3.58	17.76	4.96

reducing the intensity and sharpness of the 002 diffraction peak (Mi et al. 2015; Rizkiana et al. 2014b). On the other hand, the influence of inert ash ingredient on graphitization structure is similar to that of AAEM, but much weaker than it, implying that biomass ash can increase the defect structure of char samples.

The calculated microcrystalline structure parameters for the char samples are listed in Table 3. The stacking height $L_{c,a}$ of the AC char was 18.95 Å, and the stacking layer number N ($L_{c,a}/d_{002,a}$) was 5.23. The interplanar spacing $d_{002,a}$ of AC-CSA and AC-PSA changed slightly, while the stacking height $L_{c,a}$ and the N gradually decreased than of individual char. In addition, with increasing mass ratio of biomass ash additive from 20% to 80%, the $L_{c,a}$ and N of AC-CSA was obviously observed to decrease from 18.59 and 5.13 Å to 15.61 and 4.39 Å, respectively. Accordingly, the $L_{c,a}$ and N of AC-PSA slightly decreased from 18.69 and 5.15 Å to 17.76 and 4.96 Å, respectively. Considering the qualitatively and quantitatively results, the biomass ash addition was unfavorable for the growth of adjacent basic structural units (BSUs) in a vertical direction of the carbon structure, indicating that it was conducive to slowing down the graphitization process of the char samples (Wei et al. 2018). Moreover, the inhibition effect on the graphitization process became more significant with the rise of the biomass ash mass ratio. Meanwhile, it's worth noting that the inhibition effect of the CSA on the AC sample was higher than that of PSA at the same mixing mass ratio during pyrolysis. This expected conclusion was mainly attributed to the different chemical composition between CSA and PSA. It could be observed from Table 3 that CSA had higher active contents (potassium and sodium) and lower inert content (silicon) and active content (calcium) than PSA. Yip et al. (2010) concluded that K had the strongest inhibition effect on the graphitization process during the pyrolysis process. Consequently, the CSA additive led to the lower graphitization degree than that of PSA during the AC pyrolysis process.

3.2 Influence of biomass ash on the CO₂ gasification reactivity of AC sample

Figure 4 presented the gasification characteristic curve of the AC char, AC-CSA and AC-PSA char samples with different mass ratio at 900 °C. As observed in Fig. 4, for the same time, the carbon conversion of AC char was lower than those of mixed chars with biomass ash additives.

The reactivity parameters from Fig. 5 also obviously showed the gasification reactivity order of char samples were: AC-CSA80% > AC-CSA50% > AC-CSA20% > AC char and AC-PSA80% > AC-PSA50% > AC-PSA20% > AC char. The phenomena meant both of the biomass ash additives were conducive to improving the gasification reactivity. As we know, the structural characteristics of char were the essential influence factors for the CO₂ gasification reactivity. As mentioned above, the graphitization degree was reduced by the biomass ash additive, indicating that more structural defects of various forms were formed in the char samples (Wei et al. 2019). Hence, it was beneficial for increasing the amorphous carbon of AC char, and then promoting the gasification reactivity. On the other hand, the biomass ash additive might provide abundant pore structure of AC sample during the coal pyrolysis process, implying that the penetration resistance of CO₂ gasifying agent into the reaction sites on the char surface was reduced during the gasification process. Accordingly, the number of active sites in the carbon matrix was increased. The comprehensive analysis of the two aspects suggested that the biomass ash additive led to the structural reforming of char, and then promoted the gasification reactivity. Meanwhile, compared Fig. 4a with 4b, it could be obviously observed that the promoting effect of CSA on the reactivity was higher than that of PSA. Accordingly, as shown in Fig. 5, different reactivity parameters of AC-CSA were much larger than that of AC-PSA. The conclusion that potassium, sodium, and calcium were the crucial catalytic species for gasification reactivity in the char samples during the whole gasification process
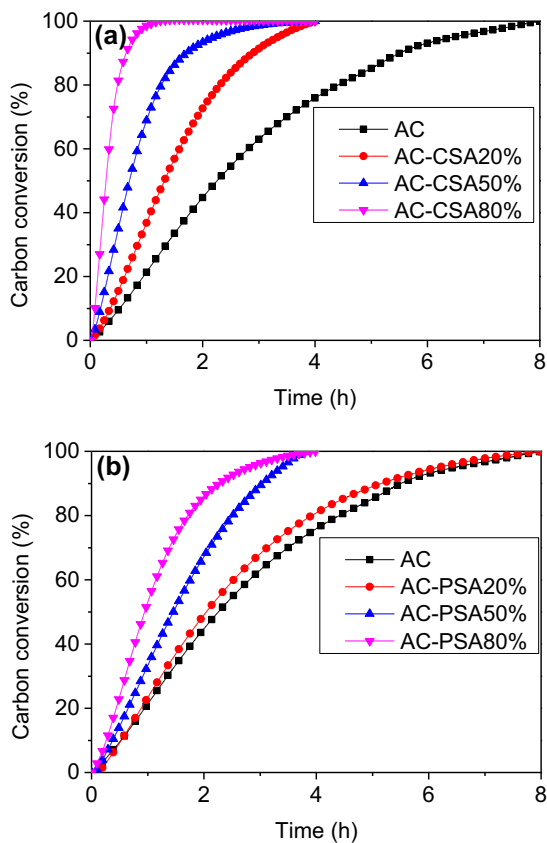
Fig. 4 Carbon conversion versus reaction time of char samples during CO_2 gasification: **a** AC-CSA char, **b** AC-PSA char

has been drawn by Yip et al. (2010) and Zhang et al. (2010). Additionally, Yip et al. (2010) and Huang et al. (2009) put forward that the catalytic performance order of various AAEM catalysts on gasification reactivity was K > Na > Ca. Therefore, except for a lower degree of graphitization of AC-CSA char samples, the higher active contents (especially K and Na) of AC-CSA chars played a significant catalytic role in the gasification process. Overall, the abundant active AAEM (especially K and Na) contents and a lower degree of graphitization jointly promoted the gasification performance.

3.3 Correlation between microstructure characteristics and gasification reactivity of char samples

Given the crystalline structure parameters usually could be employed to reflect the microstructure characteristics of char samples, the correlation between crystalline structure parameters and reactivity parameters should be established to further explore the influence of ash additive on the gasification characteristic. It's worth noting that different reactivity parameters represent the various reaction stages. As shown in Fig. 6, the reaction rate first increased and then decreased, indicating that gasification process could be divided into three stages (Liu et al. 2020b). At the initial stage, the reactive carbon preferred to react with CO_2. As the reaction progressed, some closed pores were opened and then more pore surface was created. It has been
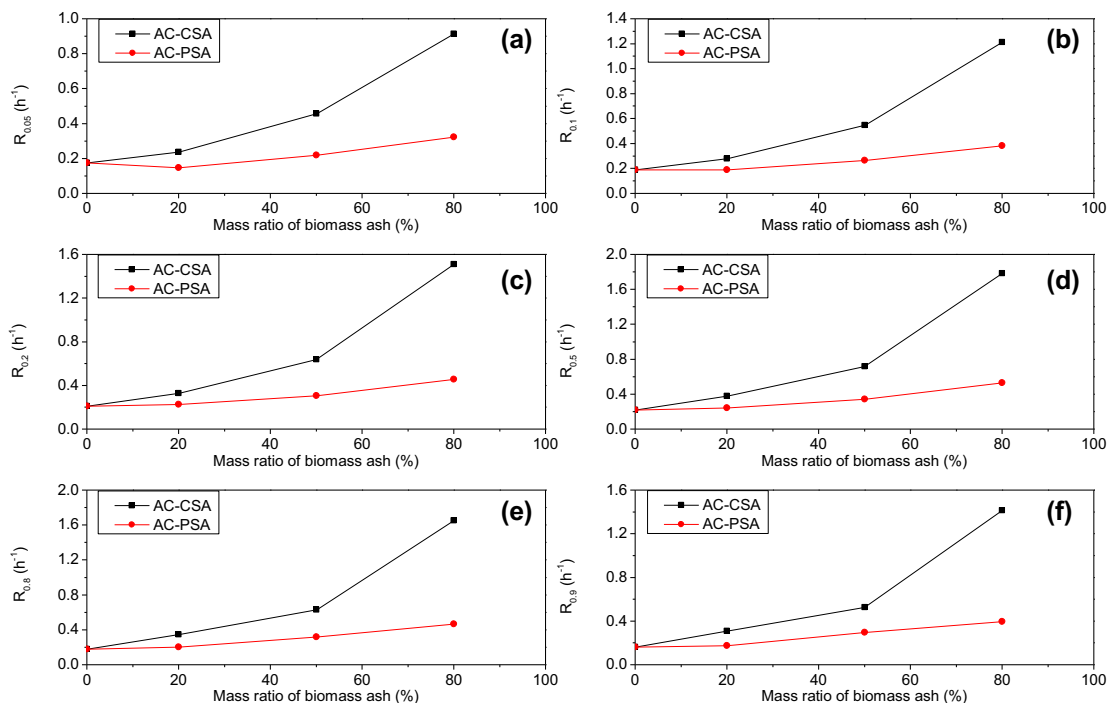
Fig. 5 Reactivity parameters of different char samples: **a** $R_{0.05}$, **b** $R_{0.1}$, **c** $R_{0.2}$, **d** $R_{0.5}$, **e** $R_{0.8}$, **f** $R_{0.9}$
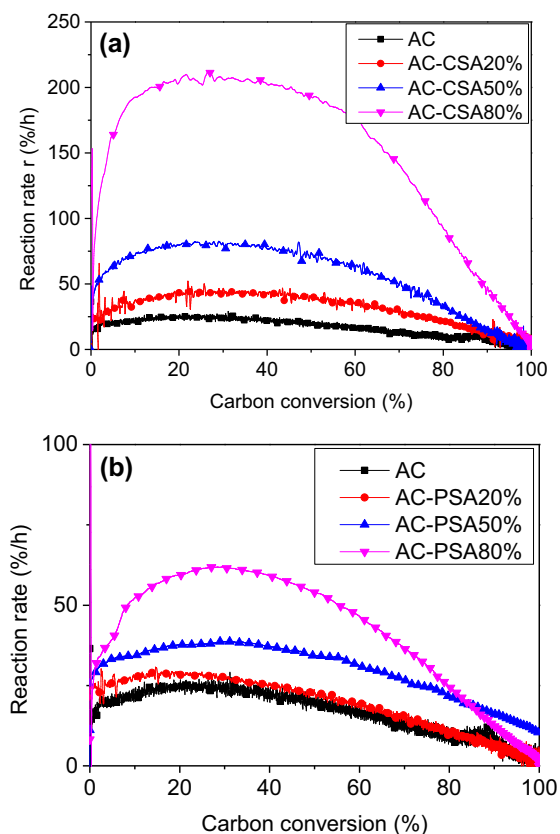
Fig. 6 Carbon conversion and reaction rate curve of char samples: a AC-CSA char, b AC-PSA char

generally accepted that the pore structure of coal char acts as a channel connecting with char and gasifying agent, which affects the diffusion of gasifying agent and gasification products during the whole gasification process. Accordingly, developed pore structure is conductive to the mass transfer of reactants and products, indicating that it will enhance the char reactivity (Adschiri and Furusawa 1986). Meanwhile, the pore structure plays a substantial role in providing the active site as the reaction interface between gasifying agent and coal char (Hurt et al. 1991). Hence, the gasification rate gradually increased and reached the maximum. When the reaction carried on, the carbon was continuously consumed, and the pore might collapse. Therefore, the reaction rate gradually decreased at the final stage. It seems that a single reactivity parameter could not precisely evaluate the whole gasification process. The correlations between stacking layer number N and different reactivity parameters of char samples using linear regression model were proposed in this investigation. The relationship between other crystalline structure parameters (stacking height $L_{c,a}$ and interplanar spacing $d_{002,a}$) and different reactivity parameters presented slightly low correlation coefficients compared with that of N. Then, Fig. 7 was taken as an example to elucidate the correlation

between microstructure of char samples and gasification performance at various reaction stage.

As shown in Fig. 7, it could be observed that gasification reactivity of char samples had the negative correlations with N, indicating that N had negative influence on the evolution of char reactivity. Meanwhile. The excellent linear correlations between N and different reactivity parameters ($R_{0.05}$, $R_{0.1}$, $R_{0.2}$, $R_{0.5}$, $R_{0.8}$, and $R_{0.9}$) were found. By comparing the correlation coefficients, it could be found the linear correlation model between $R_{0.05}$ and N had the lowest correlation coefficient, while the correlation coefficient of $R_{0.5}$, $R_{0.8}$, and $R_{0.9}$ was basically same. As mentioned above, the reaction rate varied with the progress of the gasification reaction. Especially, insufficient CO_2 concentration could seriously affect the determination of gasification reactivity results at low carbon conversion but slightly affect the results at high carbon conversion, which could be attributed to the gas switching under isothermal gasification. Meanwhile, various carbon structure forms (amorphous carbon and graphite-like structure) might have different activity energy reacting with CO_2. The role of graphite-like structure was more likely to be present in the later stage of the gasification reaction. The stacking layer number N could represent the graphite-like structure to some extent. Therefore, N could reasonably characterize the evolution of char microstructure, and reasonably predicted the change trend of reactivity parameters ($R_{0.5}$, $R_{0.8}$, and $R_{0.9}$) under the experimental conditions. However, coal char is a typical example of highly heterogeneous and complicated material, and the coal char reactivity is also influenced by the AAEMs, physical structure, and gasification conditions, thus the prediction models based on the char structure for evaluating the char reactivity need further explore.

4 Conclusions

In this study, the influence of biomass ash in coal-biomass ash mixtures during pyrolysis and gasification were explored. The structural characteristics of Jincheng AC char and mixed char samples of two biomass ash addition with different mass ratios were analyzed with the help of XRD. The resultant chars were isothermally gasified with CO_2 at 900 °C. The main conclusions were made as follows:

(1) Both CSA and PSA additives slowed down the graphitization process of the anthracite during pyrolysis, indicating that more disordered carbon structure was formed than AC char. Accordingly, the stacking height $L_{c,a}$ and stacking layer number N of AC-CSA significantly decreased with increasing
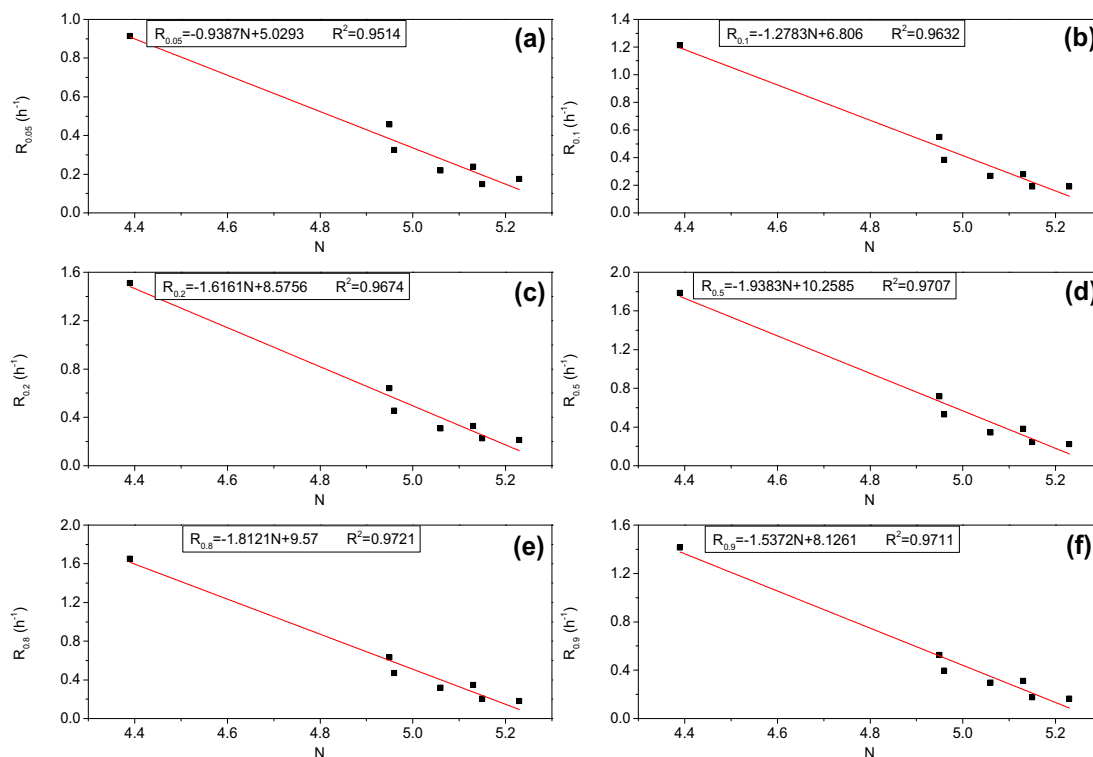
Fig. 7 Correlation between N and different reactivity parameter of char samples: **a** $R_{0.05}$, **b** $R_{0.1}$, **c** $R_{0.2}$, **d** $R_{0.5}$, **e** $R_{0.8}$, **f** $R_{0.9}$

mass ratio of biomass ash additive from 18.95 and 5.23 Å to 15.61 and 4.39 Å, respectively. Also, the $L_{c,a}$ and N of AC-PSA slightly decreased to 17.76 and 4.96 Å, respectively. The inhibition effect was gradually promoted with increasing mass ratio of biomass ash from 0% to 80%.

(2) Abundant active AAEM (especially K and Na) contents of biomass ash and a lower graphitization degree of mixed chars could be responsible for the fact that the addition of CSA and PSA improved the reactivity parameter $R_{0.5}$ (as an example) of anthracite char gasification from 0.2215 to 1.7857 and 0.5319 h^{-1}, respectively, indicating that the gasification reactivity of AC char sample was prominently promoted.

(3) Higher K and Na contents illustrated that the CSA presented more remarkable promotion effect on reactivity and the inhibition effect on the order degree of anthracite char than PSA.

(4) The excellent linear correlations ($R^2 > 0.97$) between the stacking layer number N and gasification reactivity parameters ($R_{0.5}$, $R_{0.8}$, and $R_{0.9}$) of the char samples were established, respectively.

Authors' contributions Xiaoming Li: Conceptualization, Methodology, Writing—review and editing. Caifeng Yang: Visualization, Investigation. Mengjie Liu: Data curation, Writing—original draft. Jin Bai: Supervision, Validation, Writing—review and editing. Wen Li: Supervision, Validation.

Compliance with ethical standards

References

Adschiri T, Furusawa T (1986) Relation between CO_2 reactivity of coal char and BET surface area. Fuel 65(7):927–931

Bo F, Bhatia SK, Barry JC (2003) Variation of the crystalline structure of coal char during gasification. Energy Fuels 17(3):744–754

Carpenter D, Westover TL, Czernik S, Jablonski W (2014) Biomass feedstocks for renewable fuel production: a review of the impacts of feedstock and pretreatment on the yield and product distribution of fast pyrolysis bio-oils and vapors. Green Chem 16(2):384–406

Ding L, Zhou Z, Guo Q, Huo W, Yu G (2015) Catalytic effects of Na_2CO_3 additive on coal pyrolysis and gasification. Fuel 142:134–144

Fernandes R, Hill JM, Kopyscinski J (2017) Determination of the synergism/antagonism parameters during co-gasification of potassium-rich biomass with non-biomass feedstock. Energy Fuels 31(2):1842–1849

Huang Y, Yin X, Wu C, Wang C, Xie J, Zhou Z, Ma L, Li H (2009) Effects of metal catalysts on CO_2 gasification reactivity of biomass char. Biotechnol Adv 27(5):568–572

Hurt RH, Sarofim AF, Longwell JP (1991) The role of microporous surface area in the gasification of chars from a sub-bituminous coal. Fuel 70(9):1079–1082

Karimi A, Gray MR (2011) Effectiveness and mobility of catalysts for gasification of bitumen coke. Fuel 90(1):120–125

Kopyscinski J, Rahman M, Gupta R, Mims CA, Hill JM (2014) K_2CO_3 catalyzed CO_2 gasification of ash-free coal. Interactions of the catalyst with carbon in N_2 and CO_2 atmosphere. Fuel 117(1):1181–1189

Li R, Zhang J, Wang G, Ning X, Wang H, Wang P (2017) Study on CO_2 gasification reactivity of biomass char derived from high-temperature rapid pyrolysis. Appl Therm Eng 121:1022–1031

Liu X, Xiong B, Huang X, Ding H, Zheng Y, Liu Z, Zheng C (2017) Effect of catalysts on char structural evolution during hydro-gasification under high pressure. Fuel 188:474–482

Liu M, Bai J, Kong L, Bai Z, He C, Li W (2020a) The correlation between coal char structure and reactivity at rapid heating condition in TGA and heating stage microscope. Fuel 260:11638

Liu M, Bai J, Yu J, Kong L, Bai Z, Li H, He C, Ge Z, Cao X, Li W (2020b) Correlation between char gasification characteristics at different stages and microstructure of char by combining x-ray diffraction and raman spectroscopy. Energy Fuels 34(4):4162–4172

Masnadi MS, Grace JR, Bi XT, Lim CJ, Ellis N (2015) From fossil fuels towards renewables: inhibitory and catalytic effects on carbon thermochemical conversion during co-gasification of biomass with fossil fuels. Appl Energy 140:196–209

Mi J, Wang N, Wang M, Huo P, Liu D (2015) Investigation on the catalytic effects of AAEM during steam gasification and the resultant char reactivity in oxygen using Shengli lignite at different forms. Int J Coal Sci Technol 2(3):223–231

Qin Y, Han Q, Zhao Z, Du Z, Feng J, Li W, Vassilev SV, Vassileva CG (2017) Impact of biomass addition on organic structure and mineral matter of char during coal-biomass co-gasification under CO_2 atmosphere. Fuel 202:556–562

Qing M, Su S, Chi H, Xu J, Sun Z, Gao J, Xu K, Hu S, Wang Y, Hu X, Xiang J (2019) Relationships between structural features and reactivities of coal-chars prepared in CO_2 and H_2O atmospheres. Fuel 258:116087

Rizkiana J, Guan G, Widayatno WB, Hao X, Huang W, Tsutsumi A, Abudula A (2014a) Effect of biomass type on the performance of co-gasification of low rank coal with biomass at relatively low temperatures. Fuel 134:414–419

Rizkiana J, Guan G, Widayatno WB, Hao X, Li X, Huang W, Abudula A (2014b) Promoting effect of various biomass ashes on the steam gasification of low-rank coal. Appl Energy 133:282–288

Satyam Naidu V, Aghalayam P, Jayanti S (2016) Synergetic and inhibition effects in carbon dioxide gasification of blends of coals and biomass fuels of Indian origin. Bioresour Technol 209:157–165

Sermyagina E, Saari J, Kaikko J, Vakkilainen E (2016) Integration of torrefaction and CHP plant: operational and economic analysis. Appl Energy 183:88–99

Vassilev SV, Baxter D, Andersen LK, Vassileva CG (2013) An overview of the composition and application of biomass ash. Part 1. Phase-mineral and chemical composition and classification. Fuel 105:40–76

Wei J, Gong Y, Guo Q, Ding L, Wang F, Yu G (2017a) Physicochemical evolution during rice straw and coal co-pyrolysis and its effect on co-gasification reactivity. Bioresour Technol 227:345–352

Wei J, Guo Q, Gong Y, Ding L, Yu G (2017b) Synergistic effect on co-gasification reactivity of biomass-petroleum coke blended char. Bioresour Technol 234:33–39

Wei J, Gong Y, Ding L, Yu J, Yu G (2018) Influence of biomass ash additive on reactivity characteristics and structure evolution of coal char-CO_2 gasification. Energy Fuels 32(10):10428–10436

Wei J, Guo Q, Ding L, Gong Y, Yu J, Yu G (2019) Understanding the effect of different biomass ash additions on pyrolysis product distribution, char physicochemical characteristics, and char gasification reactivity of bituminous coal. Energy Fuels 33(4):3068–3076

Wu S, Jing G, Xiao Z, Wu Y, Gao J (2008) Variation of carbon crystalline structures and CO_2 gasification reactivity of Shenfu coal chars at elevated temperatures. Energy Fuels 22(1):199–206

Wu Z, Yang W, Meng H, Zhao J, Chen L, Luo Z, Wang S (2017) Physicochemical structure and gasification reactivity of co-pyrolysis char from two kinds of coal blended with lignocellulosic biomass: effects of the carboxymethylcellulose sodium. Appl Energy 207:96–106

Wu Z, Ma C, Jiang Z, Luo Z (2019) Structure evolution and gasification characteristic analysis on co-pyrolysis char from lignocellulosic biomass and two ranks of coal: effect of wheat straw. Fuel 239:180–190

Xie Y, Yang H, Zeng K, Zhu Y, Hu J, Mao Q, Liu Q, Chen H (2019) Study on CO_2 gasification of biochar in molten salts: reactivity and structure evolution. Fuel 254:115614

Yip K, Tian F, Hayashi J-I, Wu H (2010) Effect of alkali and alkaline earth metallic species on biochar reactivity and syngas compositions during steam gasification. Energy Fuels 24(1):173–181

Zhang Y, Hara S, Kajitani S, Ashizawa M (2010) Modeling of catalytic gasification kinetics of coal char and carbon. Fuel 89(1):152–157

Zhang S, Dong Q, Chen T, Xiong Y (2016a) Combination of light bio-oil washing and torrefaction pretreatment of rice husk: its effects on physicochemical characteristics and fast pyrolysis behavior. Energy Fuels 30(4):3030–3037

Zhang S, Dong Q, Zhang L, Xiong Y (2016b) Effects of water washing and torrefaction on the pyrolysis behavior and kinetics of rice husk through TGA and Py-GC/MS. Bioresour Technol 199:352–361

Zhang K, Wang Z, Fang W, He Y, Hsu E, Li Q, Gul-e-Rana J, Cen K (2019) High-temperature pyrolysis behavior of a bituminous coal in a drop tube furnace and further characterization of the resultant char. J Anal Appl Pyrol 137:163–170

Zheng P, Wang Y, Liu C, Guo W, Bai L, Hu X, Lin X (2019) Effects of inherent alkali and alkaline earth metals on nitrogen

transformation during steam gasification of Shengli lignite. Int J Coal Sci Technol 6(2):197–206

Zhou H, Sha Y, Xiao Z, Li L, Hao J, Yang K, Li N, He R, Liu Q (2018) Using benzene carboxylic acids to prepare zirconium-based catalysts for the conversion of biomass-derived furfural. Int J Coal Sci Technol 5(4):464–472

Zhu H, Wang X, Wang F, Yu G (2018) In situ study on K_2CO_3-catalyzed CO_2 gasification of coal char: interactions and char structure evolution. Energy Fuels 32(2):1320–1327